



# 2D Potential Flow Stability Calculation in Interacting Sails for Ships

Pradeep Arun G<sup>1</sup>, Clinton paul<sup>2</sup>, Ahammed Ramshad K<sup>3</sup>

UG Scholar, Department of Marine Engineering<sup>1, 2, 3</sup>

PSN College of Engineering & technology, Tirunelveli, India<sup>1, 2, 3</sup>

**Abstract**—Ship sail-assisting is a kind of integrated technology involved in fluent dynamic analysis, sail structure design, sail rotation control, ship stability and maneuverability. This paper systematically introduces several aspects of sail-assisting technology. The paper firstly introduces sail type selection and experimental results of arc sail models. Thrust force coefficient, drifting force coefficient, lifting force coefficient, resistance coefficient and rotating torque coefficient of the sail model are discussed and optimal sail rotated angle is calculated in the paper. A control mechanism and the material of sail structure are designed for the sail operation of an ocean-going bulk carrier. Based on stability requirements of ocean-going ships, this paper proposes a stability criterion for sail-assisted ships and suggests a calculation method of stability parameter for the requirements. Comments and recommendations are finally discussed for the further application of the sail onboard ship.

**Index Terms**—Arc sail Design; Sail-Assisted Ship; Ship Stability Criterion; Ship Stability Calculation; Wind Heeling Moment; Wind Tunnel Test

## I. INTRODUCTION

Sails have been utilized for ship propulsion even from ancient times, but modern sail-assisting technology was put into use only from 1970's due to the first global oil crisis. Relevant research work was carried out all over the world, especially in Germany and Japan. The first sail-assisted oil tanker was made by Japan with two rigid arc sails of 8.0 meters wide and 12.5 meters high. This ship is the first modern sail-assisted ship in the world (Meng W. M., Zhao J. H., Huang L. Z. 2009), which could save 15% energy consumption. Since 21st century with the rising of petroleum price and the drying up of fossil fuel as well as the concerning on environment protection, sail assisted propulsion plants has again become a hot topic in shipping industry with the advantage of energy saving and environment protection. The energy saving rate of current sail-assisted ship is about 5% -15% (Meng W. M., Zhao J. H., Huang L. Z. 2009). How to improve the performance of sails is a major concern in the application of sail-assisting technology.

Sail-assisting technology has been rapidly developed in the last two decades under the requirement of energy conservation and emission reduction. Aerodynamics of different sails, including sail aerodynamic forces and sail-hull

interaction were investigated (Gerhardt F., Flay R. G. J., Richards P. J. 2011). But sail-assisting technology is related with several technical respects including aerodynamic analysis of sail, sail structure design, ship stability calculation and ship maneuverability enhancement. These respects all have influences on the performance of sails and energy-saving effect. This paper systematically introduces our research work into the sail-assisting technology for ocean-going ships in the past 5 years including sail type selection, wind tunnel tests, optimal sail angle calculation, sail structure design and ship stability criterion.

## II. TYPE SELECTION AND WIND TUNNEL TEST OF SAIL MODEL

### A. The sail types for Ocean-Going Ships

There are many types of sail with different characteristics such as square sail and spinnaker in terms of shape, soft and hard sail in terms of material, laminar flow, circular, arc and SY type in terms of cross section of sail. Some other types of sail have been patented such as skysail, frat to air-duct and airfoil sail.

Following aspects should be taken into account for the sail type selection of ocean-gonging ships as:

- Good thrust performance and high energy efficiency;
- Simple structure, light weight and high intensity;
- Able to adapt to different weather conditions and could withstand sunshine and seawater erosion.
- Flexible and easy to be lifted and rotated freely around mast. Small space occupation of the ship. No electromagnetic interference to the instrumentation onboard.

According to the latest research the arc-shaped rigid sail is believed to be the best choice to meet the requirements mentioned above, due to its good aerodynamic performance, economical benefits, long duration and easy manufacture. Christo Ananth et al. [3] proposed a system, this fully automatic vehicle is equipped by micro controller, motor driving mechanism and battery. The power stored in the battery is used to drive the DC motor that causes the movement to AGV. The speed of rotation of DC motor i.e.,



velocity of AGV is controlled by the microprocessor controller. This is an era of automation where it is broadly defined as replacement of manual effort by mechanical power in all degrees of automation. The operation remains an essential part of the system although with changing demands on physical input as the degree of mechanization is increased.

A kind of rigid arc sail was selected with five different sail parameters (named as A, B, C, D and E). Wind tunnel tests were made in order to study their aerodynamic performance. The structure of rigid arc sail is shown in Fig.1.

Two parameters were defined to describe the structure of the arc sail as:

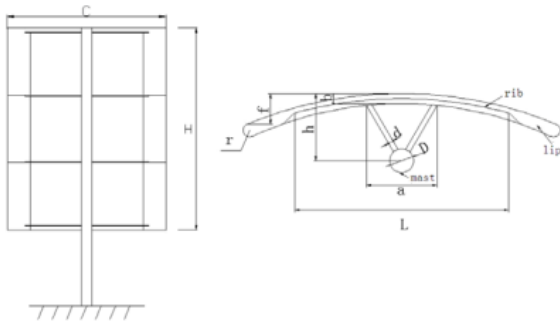


Fig. 1 The Structure Of Arc-Shaped Rigid Sail

Aspect Ratio  $\lambda$ : the specific value between height  $H$  and width  $C$  of the sail.

Here

$$\lambda = H / C$$

Camber Ratio  $f$ : the specific value between thickness  $f$  and width  $C$  of the sail.

Here

$$\tilde{f} = f / C$$

Serial number and corresponding parameters of the sails are shown in Table 1.

Table 1 The Sails Parameters

| Number                   | A    | B    | C    | D    | E    |
|--------------------------|------|------|------|------|------|
| Aspect Ratio $\lambda$   | 1.45 | 1.25 | 1.45 | 1.65 | 1.45 |
| Camber Ratio $\tilde{f}$ | 0.10 | 0.12 | 0.12 | 0.12 | 0.14 |

### B. Force Analysis of Sail Model

When a sail-assisted ship is navigating at a certain speed  $V_c$  and direction  $X$  at sea, wind will act on the sail as shown in Fig. 2.

The aerodynamic forces acting on the sail model are decomposed as forces and momentum in wind-axis coordinate system as shown in FIG.2. The wind-axis coordinate system is a rectangular coordinate system O-LDZ with axis D along relative wind direction and Z as a vertical axis. The center of the model bottom is the coordinate origin O. Here the axis L indicates the wind lifting force while axis D

indicates wind resistant force. So the aerodynamic wind forces acting on the sail could be decomposed as resistance  $FD$  with the same direction as airflow, lifting force  $FL$  perpendicular to the airflow and rotating torque  $M$  acting on the mast, where the reference point of the torque is coordinate origin O.

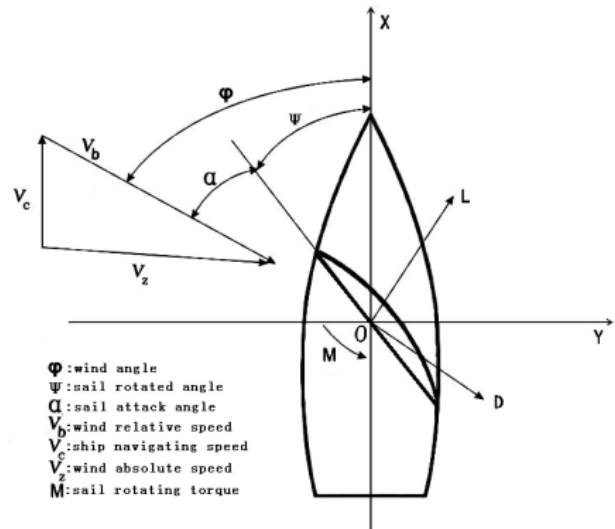


Fig. 2 The Forces Acting On The Sail

The lifting force  $FL$ , resistant force  $FD$  and rotating torque  $M$  could be expressed in terms of dimensionless index. The lifting force coefficient of the sail is as:

$$C_L = \frac{F_L}{\frac{1}{2} \rho_0 V_b^2 S}$$

Resistance force coefficient of the sail is as:

$$C_D = \frac{F_D}{\frac{1}{2} \rho_0 V_b^2 S}$$

Rotating torque coefficient of the sail is as:

$$C_m = \frac{M}{\frac{1}{2} \rho_0 V_b^2 S C}$$

### C. Wind Tunnel Test

A wind tunnel was used in the tests, which is a suction-type, slow-speed, direct-current wind tunnel. The length of tunnel is 14 m and the sectional area of which is square. The tested wind speed could be adjusted continuously between 2 m/s and 30 m/s. The contraction ratio is 3.56 and the turbulence scale is blew 1%. As a 90kW DC fan system is controlled by a computer, the wind speed could be adjusted and controlled easily and accurately. It was discussed in the previous work that Christo Ananth et al. [5] proposed a system, this fully automatic vehicle is equipped by micro controller, motor



driving mechanism and battery. The power stored in the battery is used to drive the DC motor that causes the movement to AGV. The speed of rotation of DC motor i.e., velocity of AGV is controlled by the microprocessor controller. This is an era of automation where it is broadly defined as replacement of manual effort by mechanical power in all degrees of automation. The operation remains an essential part of the system although with changing demands on physical input as the degree of mechanization is increased.

The wind tunnel is equipped with a turning disc, which is controlled by the computer. The rotation angle is used to simulate different angles between air flow and sail model. The main instrumentation used in the sail model dynamometry test is as following.

- velocity pressure sensor (500Pa)
- bottom-supported five-component strain-gauge force balance
- DH5920 dynamic signal measurement and analysis system
- NI sampling and data acquisition system

On this occasion that force measurement range is 100 N, the static calibration accuracy of the aerodynamic measuring system is 0.3% with 100 N force range, 50 N.m bending range and 10 N.m torque range.

The dynamometry test of sail model was carried out in a uniform flow field (the wind speed is 15 m/s) and the dimensionless values of lifting force, resistance and the torque for the five thin-wing arc sails A,B,C,D and E were recorded. The range of sail attack angle is between  $-5^\circ$  and  $90^\circ$  with measuring interval of  $5^\circ$ . The Aerodynamic results for each of the sail models like lifting force coefficient  $CL$ , resistance coefficient  $CD$  and torque coefficient  $Cm$  are shown as Fig. 3, Fig.4, Fig.5 respectively.

Lift coefficient is closely related to camber of the sail, while drag coefficient is influenced by sail surface condition and air separation behind the sail. As seen from the curves with different aspect ratios and different camber ratios of the five sail models, the lifting coefficients, resistance coefficients and torque coefficients all demonstrate the same variation tendency. The lift coefficient and drag coefficient curves are consistent with the general law of aerodynamic performance of the arc sail.

When the sail attack angle is between  $0^\circ$  and  $30^\circ$ , the  $CL$  and  $CD$  have positive correlation and  $CL$  has higher changing rate. When the sail attack angle reaches to a certain value (around  $30^\circ$ ),  $CL$  will reach to its extreme, namely the inflection at a turning point of the curve. Then  $CL$  begins to decrease rapidly while  $CD$  continues to increase.  $CL$  has a negative correlation while  $CD$  has a positive correlation and with  $\alpha$ .

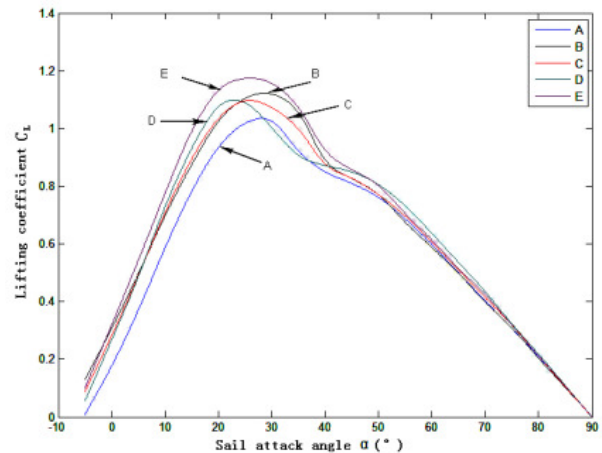


Fig. 3 Lifting Coefficients with Different Attack Angle

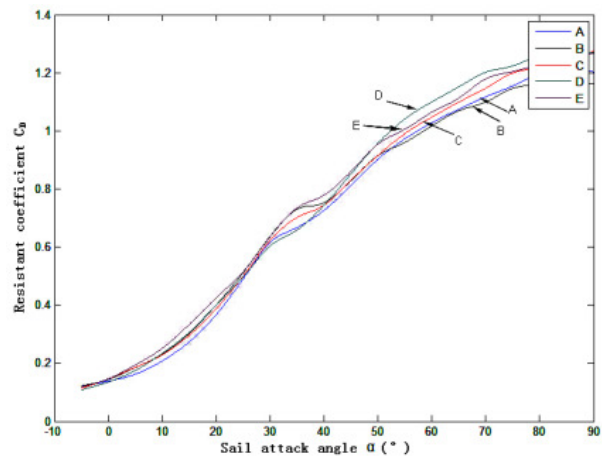


Fig. 4 Resistant Coefficient with Different Attack Angle

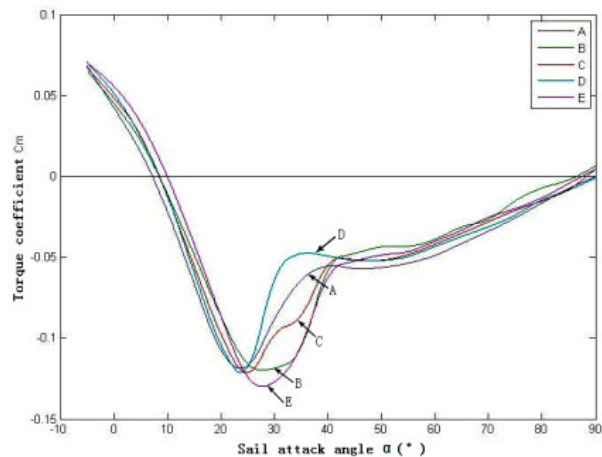


Fig. 5 Torque Coefficients with Different Attack Angle

Because the arc sail has similar working principle to the wing aerodynamics, the inflection point occurring on the  $CL-\alpha$  curve is called a stall. This is due to that under larger sail attack angle, vortex separation will take place behind the sail. From  $Cm-\alpha$  curve it could be seen that  $Cm$  reaches its



minimum at the inflection point of the  $CL-\alpha$  curve. Here the force acting on the sail reaches to the maximum, namely, the load of the sail also reaches to the maximum. Judged from the wind tunnel test results of the five sail models, the sail model E could have the best aerodynamic performance for ocean-going ships.

#### D. Force Acting on Ships

Actually the forces acting on ships are thrust force  $T$  and drifting force  $H$ , which could be derived from the lifting force  $FL$  and resistant force  $FD$  of the sail.

$$T = F_L \sin \phi - F_D \cos \phi$$

$$H = F_L \cos \phi + F_D \sin \phi$$

The thrust force  $T$  and drifting force  $H$  could be expressed in the terms of dimensionless index as:

$$C_T = C_L \sin \phi - C_D \cos \phi$$

$$C_H = C_L \cos \phi + C_D \sin \phi$$

Where:

Thrust force Coefficient of the wind:

$$C_T = \frac{T}{\frac{1}{2} \rho_0 V_b^2 S}$$

Drifting Force Coefficient of the wind:

$$C_H = \frac{H}{\frac{1}{2} \rho_0 V_b^2 S}$$

According to formula (6), (7) and the wind tunnel test results, the maximum thrust coefficient and the corresponding drifting force coefficient of the sail model E was calculated against different wind angles  $\phi$ . Hence the viable sail operation range is between  $30^\circ$  and  $180^\circ$  and the maximum thrust coefficient curve was obtained as shown in Fig.6. The optimal sail angle and the optimal sail rotated angle are shown in Fig. 7 and Fig. 8 respectively.

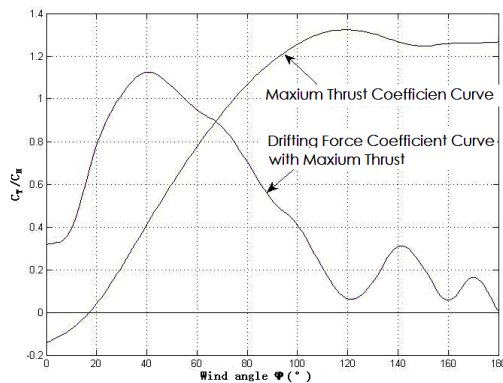


Fig. 6 Thrust Coefficients and Drifting Coefficient With Different Wind Angle

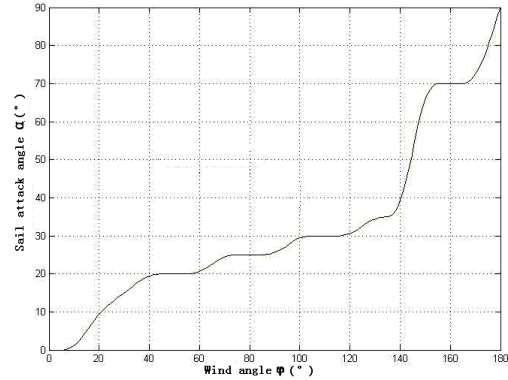


Fig. 7 Optimal Sail Attack Angle with Different Wind Angle

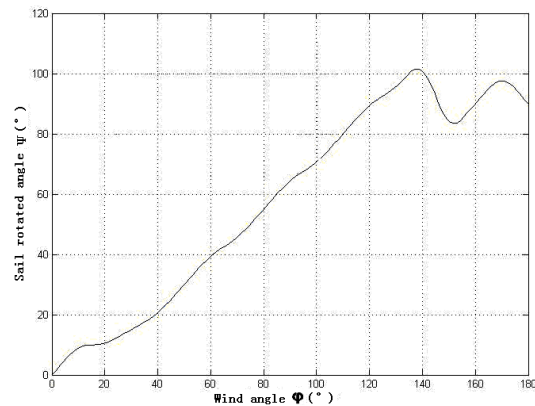


Fig. 8 Optimal Sail Rotated Angle with Different Wind Angle

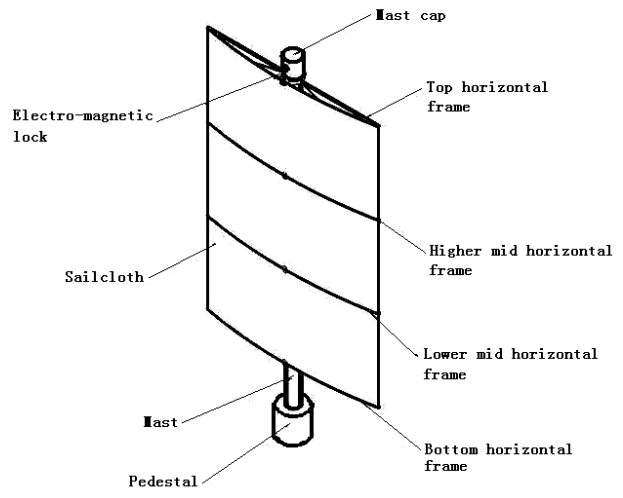


Fig. 9 Sail Structure When It Is Ascended

### III. SAIL STRUCTURE DESIGN

#### A. Basic Design Principles

The design principles of sail structure are determined by the analysis of marine wind energy, ship stability, bridge vision field and many other factors as:



a) The sail shall be able to utilize wind energy at different heights. The upper part of the sail shall be stronger than the other parts since the wind is stronger there;

b) Sail area shall be designed as large as possible on condition that the ship stability is satisfied. The sail area shall be able to be adjusted according to different wind speed to ensure the ship dynamic stability;

c) When the sail is ascended, it will not influence the vision field of Ship Bridge;

d) The occupied space of sail shall be as small as possible when it is descended.

### B. The Sail Structure

According to the principles mentioned above, a multi-segmented sail structure was designed for ocean-going ships. The sail is an arc-shaped rigid sail, which is capable of being operated like ascending, descending or rotation. The sail is composed of 3 or 4 segments, each of which could be descended separately. In this way, the height of sail could be adjusted with electro-magnetic locks in sail frames. The sail aspect ratio is 1.45 and the camber ratio is 0.14. When the sails are ascended, segments at different levels will work with the action of wind and the vision field of the bridge will not be disturbed. When the sails are descended, sails at different levels will be overlaid together, occupying small space of the ship. When it works, the sails could be rotated according to different wind direction, and the sail working area could be adjusted according to different wind speed at sea to take the best advantage of wind energy and meanwhile secure shipping safety. Axonometric view of the sail is shown in Fig. 9 when the sails are ascended. The sail structure is composed of a rotating chassis, masts, top segment, mid segments, bottom segment and other components. In addition, there are some accessories like aero-vane, actuating structure for the rotating chassis, transmission structure, locking mechanism, ropes used to ascend and descend the sails, pulleys, motors and winches, etc. (invisible in Fig. 9). As discussed in the previous work, Christo Ananth et al. [9] proposed a system, this fully automatic vehicle is equipped by micro controller, motor driving mechanism and battery. The power stored in the battery is used to drive the DC motor that causes the movement to AGV. The speed of rotation of DC motor i.e., velocity of AGV is controlled by the microprocessor controller. This is an era of automation where it is broadly defined as replacement of manual effort by mechanical power in all degrees of automation. The operation remains an essential part of the system although with changing demands on physical input as the degree of mechanization is increased.

In order to adjust height of sail, there is a electro-magnetic lock in the frame of each segment. When wind is strong enough, the lock in top horizontal frame will be unlocked and the top segment will be descended. When wind is too strong, another segment will be descended until the sail-assisted ship stability is satisfied under stronger wind.

To ascend the sail, a motor on the bottom drives the winch drum on chassis. Then the wire-rope on the winch drum is

rolled up and the sail is ascended. When the sail is aroused to a certain position, the winch is stopped and a locking mechanism which is mounted on the mast will secure the sail. The chassis will rotate the sail to an optimal sail rotated angle according to the wind direction as shown in Fig. 8.

### C. Sail Material Selection

Standards have been made for the material used in naval architecture and ocean engineering because of severe working environment at sea. The material of sail should have good mechanical characters, corrosion-resisting and economic performance. Sometimes these standards are conflicting, which need compromise between various requirements.

The nylon canvas coated with hard fiber is believed to be the most suitable material for the sail to prevent air penetration and enhance good aerodynamic performance. Generally, there are three kinds of materials suitable for sail skeleton: steel, aluminum and fiberglass. Steel material has higher strength and lower cost. But the weight of the steel is heavy unfavorable to ship stability. Aluminum material has light weight and good processing performance, but it is not suitable for large sail due to its high price and poor elasticity. Fiberglass is taken to be an ideal material for sail skeleton with its small specific gravity, high specific strength and good elasticity.

The mast is the main structure of sail. Traditional material for sail mast is wood of high quality. Because of automatic control requirement for modern sail, the wood should be replaced due to its limitations in strength and resources. Three candidate materials have been selected as shown in Table 2, including ordinary low-alloy steel, stainless steel and Glass Reinforced Plastics.

## IV. STABILITY OF SAIL-ASSISTED SHIPS

Appropriate stability, floating condition and strength must be ensured in the process of loading, transporting and unloading of ships. Due to the action of wind, sail-assisted ship has some different characteristics compared to the conventional powered ship in terms of stability. Means of correctly checking the stability of sail-assisted ship is one of major problems in the application of sail-assisting technology.

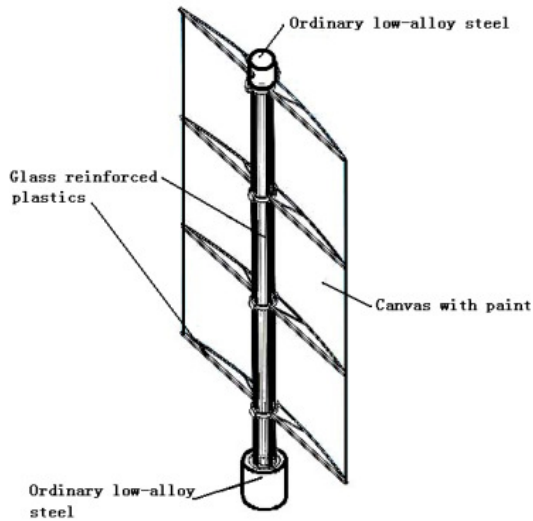


Fig. 10 Sail Structure With Different Materials

Table 2 The Comparison And Analysis For Candidate Materials

| Properties Materials      | Type                                      | Density | Yield Strength | Current Applications                                      | Comments  |
|---------------------------|---|---------|----------------|---|---|
| Ordinary Low-alloy Steel  | 16Mn(Q345)                                | 7.85    | 345            | Large Steel Structures, Bridges, Ships, Pressure Vessels. | Good Mechanical Properties, Acceptable Low Temperature Performance, Good Ductility and Weld ability |
|                           | 16MnNb (Q390)                             | 7.85    | 390            | Large Welded Parts, Pipes, Heavy Machinery and Equipment  | higher Yield Strength Than 16Mn   |
|                           | 14MnVTiRE (Q420)                          | 7.85    | 420            | Welded Components, Heavy Machinery And Equipment          | High Strength, Good Fatigue Resistance  |
| Glass Reinforced Plastics | Epoxy Glass Reinforced Plastics           | 1.73    | 520            | Main Bearing Components, Corrosion-resistant Parts        | High Cost, Poor Manufacturability, High Shrinkage   |
|                           | Polyester Resin Glass Reinforced Plastics | 1.75    | 237            | Components With General Requirements, Such as Cars, Ships | Poor Acid and Alkali Resistance   |
|                           | Phenolic Resin Glass Reinforced Plastics  | 1.8     | 110            | Aircraft Interior Decoration, Electrical Materials        | Lower Strength, Toxic   |
| Stainless Steel           | 304                                       | 7.93    | 300            | Appliance Tools   | Food grade" stainless steel   |
|                           | 316                                       | 8.03    | 315            | Marine Steel  | Good resistance to corrosion  |
|                           | 630                                       | 7.78    | 630            | Offshore Platforms, Aerospace, Food Industry              | High Strength, Hardness And Corrosion Resistance, Poor Low-temperature Resistance                   |

A. Stability Requirement on Sail Assisted Ships

The ability of a ship to return to its equilibrium position after it is displaced there from because of the external forces and external torques  $MH$  is called ship stability. Righting moment  $MR$  is an important symbol of restoration ability. Stability calculation includes calculation and check of floating condition, initial stability, stability at large angle, static stability, dynamic stability, as well as check of weather criterion.

Ship heels under the action of static stability, which means the angular velocity is zero. When  $WH$  is equal to  $WR$ , ship reaches an equilibrium state and ship stability can be measured by  $WR$ . On the contrary, if ship is heeled by external forces, only when the work done by external moment is equal to that done by righting moment, can the ship stop heeling. And the ability of a ship to resist external forces is measured by the work done by stability moment instead of static moment.

$$M_R = \Delta \cdot GZ$$

Where:

$\Delta$ —current displacement volume;

$GZ$ —vertical distance from gravity center to action line of buoyancy, in other words, righting arm, which can be classified as static stability lever and dynamic stability lever.

The recommendatory stability criterion on sail-assisted ships includes:

1. Weather Criteria  $K: K=Mq^*/M_f \geq 1$
2. Metacentric Guide  $GM: GM>0.3$

V. SAIL MODEL EXPERIMENT

Based on the calculation method proposed above, a model of sail assisted ship was made, and its stability was checked. The ship model was equipped with four sails, the two bigger ones placed fore and aft, and the rest in the middle.

The particulars of the model, sail and wind condition are listed in Table 3, Table 4 and Table 5 respectively.

TABLE 3 PARTICULARS OF THE SHIP MODEL

|         |      |
|---------|------|
| $L(m)$  | 3.00 |
| $B(m)$  | 1.00 |
| $D(m)$  | 0.52 |
| $d(m)$  | 0.18 |
| $KC(m)$ | 1.25 |
| $KB(m)$ | 0.12 |
| $BM(m)$ | 1.72 |

TABLE 4 PARTICULARS OF THE SAIL

|  |      |
|--|------|
| Width of bigger sail $B_{S1}(m)$                         | 1.00 |
| Width of smaller sail $B_{S2}(m)$                        | 0.60 |
| Height of both sail $H_S(m)$                             | 3.00 |
| Area of bigger sail $S_1(m^2)$                           | 3.00 |
| Area of smaller sail $S_2(m^2)$                          | 1.80 |
| Total area of sail $S_T(m^2)$                            | 9.60 |
| Height between sail projected area and baseline $Z_S(m)$ | 2.28 |
| Wind heeling lever of sail $Z_2(m)$                      | 2.10 |

TABLE 5 PARTICULARS OF THE WIND

|   |       |
|---|-------|
| Density of air $\rho(kg \cdot s^{-2}/m^4)$                          | 0.125 |
| Coefficient of lateral wind pressure on ship $C_{H\phi}$            | 1.25  |
| Lateral projected area of ship $A(m^2)$                             | 0.99  |
| Height between lateral projected area of ship and baseline $Z_A(m)$ | 0.35  |
| Wind heeling lever of ship $Z_1(m)$                                 | 0.17  |

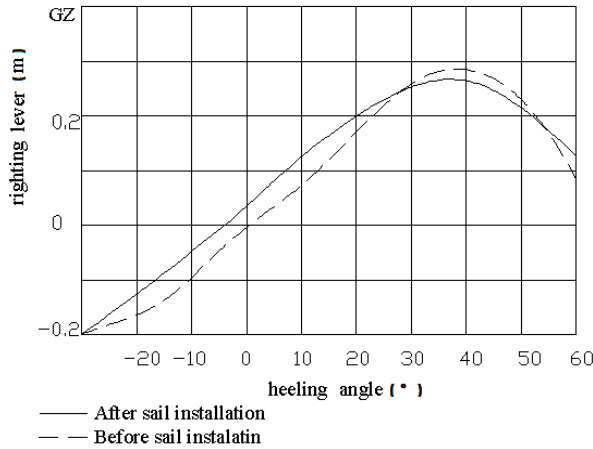


Fig. 13 Comparison Of Static Stability Curve Before Sails Installation

TABLE 6 RECORD OF THE PARAMETERS OF STABILITY

| condition                        | item | C <sub>L</sub> | C <sub>D</sub> | C <sub>M</sub> | K <sub>w</sub> | V <sub>s</sub> | M <sub>s</sub> | M <sub>0</sub> | M <sub>r</sub> | θ <sub>s</sub> |
|----------------------------------|------|----------------|----------------|----------------|----------------|----------------|----------------|----------------|----------------|----------------|
| SS <sub>x</sub> -WS <sub>y</sub> |      | 0.00           | 1.00           | 1.00           | 1.00           | 1.05           | 14.34          | 0.15           | 14.49          | 2.71           |
| SS <sub>x</sub> -WS <sub>y</sub> |      | 0.89           | 0.67           | 1.03           | 0.75           | 1.20           | 19.29          | 0.15           | 19.44          | 3.63           |
| SS <sub>x</sub> -WS <sub>y</sub> |      | 1.01           | 0.36           | 1.05           | 0.25           | 1.22           | 20.32          | 0.05           | 20.37          | 3.81           |
| SS <sub>x</sub> -WS <sub>y</sub> |      | 0.89           | 0.67           | 1.03           | 0.75           | 1.27           | 21.60          | 0.16           | 21.76          | 4.07           |
| SS <sub>x</sub> -WS <sub>y</sub> |      | 0.00           | 1.00           | 1.00           | 1.00           | 1.23           | 19.67          | 0.21           | 19.88          | 3.71           |
| SS <sub>x</sub> -WS <sub>y</sub> |      | 0.89           | 0.67           | 1.03           | 0.75           | 1.36           | 24.77          | 0.19           | 24.96          | 4.67           |
| SS <sub>x</sub> -WS <sub>y</sub> |      | 1.01           | 0.36           | 1.05           | 0.25           | 1.52           | 31.54          | 0.08           | 31.62          | 5.92           |
| SS <sub>x</sub> -WS <sub>y</sub> |      | 0.89           | 0.67           | 1.03           | 0.75           | 1.46           | 28.55          | 0.22           | 28.77          | 5.38           |
| SS <sub>x</sub> -WS <sub>y</sub> |      | 0.00           | 1.00           | 1.00           | 1.00           | 1.49           | 28.87          | 0.30           | 29.17          | 5.46           |
| SS <sub>x</sub> -WS <sub>y</sub> |      | 0.89           | 0.67           | 1.03           | 0.75           | 1.53           | 31.35          | 0.24           | 31.59          | 5.91           |
| SS <sub>x</sub> -WS <sub>y</sub> |      | 1.01           | 0.36           | 1.05           | 0.25           | 1.22           | 20.32          | 0.05           | 20.37          | 3.81           |
| SS <sub>x</sub> -WS <sub>y</sub> |      | 0.00           | 0.18           | 0.00           | 0.00           | 1.40           | 0.00           | 0.00           | 0.00           | 0.00           |
| SS <sub>x</sub> -WS <sub>y</sub> |      | 1.01           | 0.36           | 1.05           | 0.25           | 1.58           | 34.08          | 0.08           | 34.16          | 6.39           |
| SS <sub>x</sub> -WS <sub>y</sub> |      | 0.00           | 0.18           | 0.00           | 0.00           | 1.38           | 0.00           | 0.00           | 0.00           | 0.00           |
| SS <sub>x</sub> -WS <sub>y</sub> |      | 1.01           | 0.36           | 1.05           | 0.25           | 1.23           | 20.66          | 0.05           | 20.71          | 3.87           |

The height of ship gravity center after sail installation is 1.25 m, thus, the curve of static stability at light loading is redrawn. As indicated in Fig.13 the curve becomes flat after sails installation, which means that heeling moment becomes larger, and the stability condition becomes worse. Based on revised static stability curve,  $M_q$  at light loading is calculated as 40 N.m.

Tests were carried out at different angles between sail and ship, and different angles between wind and ship. Here in Table 6, SS<sub>x</sub>-WS<sub>y</sub> means that the tested angle between ship and sail is x degree, and the tested angle between wind and ship is y degree. Calculation results for the wind pressure heeling moment  $M_f$  of ship model and static Angle  $\theta_s$  are as shown in Table 6.

From the data in Table 6, some results are obtained:

- (1) The vertical height of gravity center  $GM$  is 0.59 m, which is higher than its limitation of 0.3 m;
- (2) The heeling angle  $\theta_l$  of the ship model under natural condition is 4.2 degree; the minimum overturning moment  $M_q$  is 40 N.m, which is obviously higher than the wind heeling moment  $M_f$  as shown in the Table 6;
- (3) From the Table 7, all the static Angle  $\theta_s$  are lower than 12 degree.

These results indicate that real ship model meets the stability requirements.

## VI. CONCLUSION

1. According to the wind tunnel test results, the maximum thrust coefficient and the corresponding drifting force coefficient of the sail model are between 25 ° and 45 °.

2. A multi-mast, rotary, stacking-arrangement sail structure was designed for ocean-going ships, which could be useful for improving the stability of sail-assisted ships.

3. Based on the stability criteria of ocean-going ship, this paper proposes a stability criteria for sail-assisted ship and suggests calculation methods for the stability parameter in the requirements.

4. Based on the calculation method proposed, a model of sail-assisted ship was made, and its stability was checked. The results verify that the proposed stability criteria of sail-assisted ship is feasible

## REFERENCES

- [1] Meng W. M., Zhao J. H., Huang L. Z., "Application Prospect of Sail-assisted Energy-saving Ships", Journal of Ship & Boat, 04 (2009):1-3.
- [2] Grhardt F., Flay R. G. J., Richards P. J., "Unsteady Aerodynamics of Two Interacting Yacht Sails in Two-dimensional Potential Flow", J. Fluid Mech. 668 (2011):551-581.
- [3] Christo Ananth, M.A.Fathima, M.Gnana Soundarya, M.L.Jothi Alphonsa Sundari, B.Gayathri, Praghash.K, "Fully Automatic Vehicle for Multipurpose Applications", International Journal Of Advanced Research in Biology, Engineering, Science and Technology (IJARBEST), Volume 1,Special Issue 2 - November 2015, pp.8-12.
- [4] Cleary, Chris, Daidola, John C., Reyling, Christopher J., "Sailing Ship Intact Stability Criteria", Journal of Marine Technology. 1996.
- [5] Christo Ananth, M.A.Fathima, M.Gnana Soundarya, M.L.Jothi Alphonsa Sundari, B.Gayathri, Praghash.K, "Fully Automatic Vehicle for Multipurpose Applications", International Journal Of Advanced Research in Biology, Engineering, Science and Technology (IJARBEST), Volume 1,Special Issue 2 - November 2015, pp.8-12.
- [6] Yang H., "Study on Stability of Sail Assisted Inland River Ship". In Chinese. Journal of Hunan Communication Science and Technology, 04 (1996):63-66.
- [7] Yang B. L., "Study on Stability of Sail Assisted Ships". In Chinese. Journal of Wuhan Shipbuilding, 03 (1988):22-27.
- [8] Luo H. L., Li G. L., Tan Z. S., "Stability Check of Airfoil Sail". In Chinese. Journal of South China University of Technology, 14(1986):36-40.
- [9] Christo Ananth, M.A.Fathima, M.Gnana Soundarya, M.L.Jothi Alphonsa Sundari, B.Gayathri, Praghash.K, "Fully Automatic Vehicle for Multipurpose Applications", International Journal Of Advanced Research in Biology, Engineering, Science and Technology (IJARBEST), Volume 1,Special Issue 2 - November 2015, pp.8-12.
- [10] Zhao H. L., "The Height of Gravity Center of Ships". In Chinese. Journal of Marine Technology, 03 (1997):21-23.
- [11] Shen H., Du J. L., Xu B. Z., "Calculation of Stability and Strength". In Chinese. Dalian :Dalian Maritime University Press, 2001.



Pradeep Arun G was born on 10<sup>th</sup> January 1995. He is currently a UG Scholar in PSN college of Engineering and Technology Tirunelveli, in the Department of Marine Engineering. His research areas on Ship building in the dock areas and marine related activities and auxillary engines.



Clinton Paul was born in 23<sup>rd</sup> October 1992. He is currently a UG Scholar in PSN college of Engineering and Technology Tirunelveli, in the Department of Marine Engineering. His research areas on Ship building and Ship steering and marine related activities.



Ahammed Ramshad k was born on 03<sup>rd</sup> October 1994. He is currently a UG Scholar in PSN college of Engineering and Technology Tirunelveli, in the Department of Marine Engineering. His research areas on Ship building and ship maneuverability and marine related activities.